



SAINT-VENANT DECAY RATES: A PROCEDURE FOR THE PRISM OF GENERAL CROSS-SECTION

N. G. Stephen and P. J. Wang†

Department of Mechanical Engineering, The University of Southampton, Southampton SO17 1BJ, U.K.

(Received 19 August 1994)

Abstract—A procedure previously developed for the determination of decay rates for self-equilibrated loadings at one end of a pin-jointed framework consisting of repeated identical cells, wherein the decay factors are the eigenvalues of the single cell transfer matrix, is here further developed and applied to a prismatic continuum beam of general cross-section. A sectional length of beam is treated within ANSYS finite element code as a *super element*; nodes at both ends of the section are treated as *master* nodes and the stiffness matrix relating forces and displacements at these *master* nodes is constructed within ANSYS. Manipulation of this stiffness matrix within MATLAB gives the transfer matrix from which the eigenvalues and eigenvectors may be readily determined. Accuracy of the method is assessed by treating the plane strain strip, the plane strain sandwich strip, and the rod of circular cross-section, representing a selection of the examples for which exact analytical solutions are available, and is found to be very good in all cases.

NOTATION

| | |
|---------------------|--|
| b | external radius of circular cross-section |
| c | semi-depth of plate, strip or layer |
| d | nodal displacement vector |
| e | base of Napierian logarithm |
| E | Young's modulus |
| f | volume fraction, characterizing sandwich strip |
| F | nodal force vector (according to the conventions of the finite element method) |
| G | transfer matrix |
| i | $(-1)^{1/2}$ |
| I | identity matrix |
| j, n | index of section or eigenvalue |
| k | decay rate |
| K | stiffness matrix |
| l_c | characteristic sectional length |
| m | circumferential harmonic index |
| P | nodal force vector (according to the conventions of the theory of elasticity) |
| r, θ and z | cylindrical coordinates |
| s | state vector |
| S.V.P. | Saint-Venant's principle |
| T | transpose of matrix or vector |
| u | displacement component |
| u | nodal displacement vector |
| U, V and W | displacement functions in cylindrical coordinates |
| x, y and z | Cartesian coordinates |
| λ | decay factor, eigenvalue of transfer matrix |
| ν | Poisson's ratio |

Note that the subscripts m and s denote *master* and *slave* nodes. The symbol \wedge pertains to the *super element*.

INTRODUCTION

Saint-Venant's principle (S.V.P.) underpins much of solid mechanics by allowing the replacement of an actual load system on a structural member by a statically equivalent load distributed in a particular way demanded by the elastostatic solution. The difference between the two load distributions is termed "self-equilibrating", and since it has no stress resultant or couple which requires reaction at some other location on the structure, there seems no reason why the associated stress field should penetrate any great distance into the structure. According to S.V.P. this depth of penetration should be small.

S.V.P. has been expressed and applied in a variety of ways by many authors; for example in beam problems, according to Sokolnikoff [1], "it is commonly assumed that the local eccentricities are not felt at distances that are about five times the greatest linear dimension of the area over which the forces are distributed".

The first mathematical proof of S.V.P. was provided by Toupin [2] who considered an elastic cylinder of arbitrary length and cross-section subjected to a self-equilibrated load system on one end only; Toupin demonstrated the exponential decay of elastic strain energy, and hence stress, but S.V.P. requires also that the rate of decay should be "rapid". In practice there are many examples, particularly for thin-walled structural members, where the rate of exponential decay is so slow that S.V.P. cannot really be said to apply. One example is the effect of (self-equilibrated) longitudinal warping restraint during torsion, when it is necessary to introduce the

† Visiting Research Fellow from Department of Mechanical Engineering, Shanghai Maritime Institute, Shanghai, 200135, Peoples Republic of China.

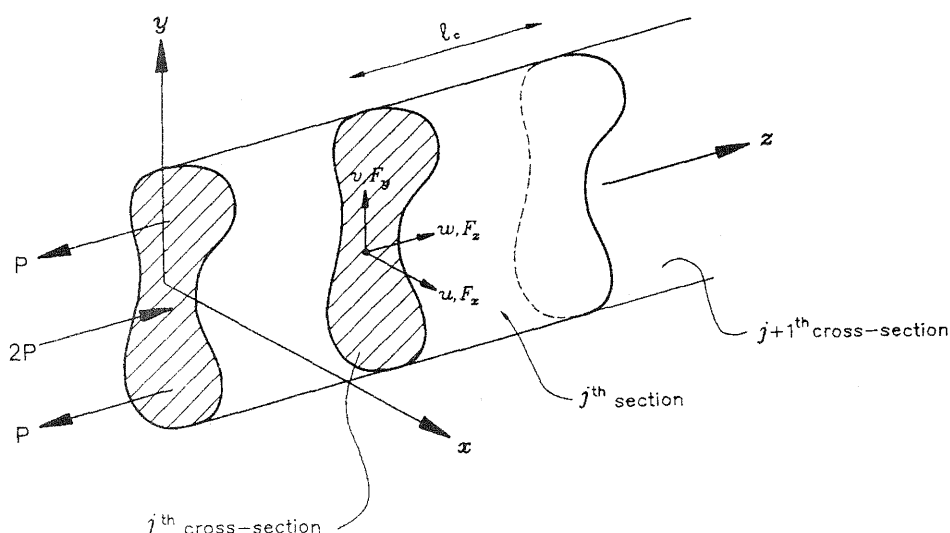


Fig. 1. Semi-infinite prismatic elastic cylinder of arbitrary cross-section subjected to self-equilibrated loading on the end $z = 0$.

bimoment [3] in order to provide a plausible engineering theory.

The vast majority of published results pertaining to S.V.P. (see recent reviews by Horgan and Knowles [4] and Horgan [5]) have concentrated on *continuum* structural members, including isotropic, anisotropic and composite structures, and the majority of the results described in Refs [4] and [5] pertain to strain energy inequalities related to stress decay.

However in a recent paper [6] the present authors described a procedure for the calculation of the exact rates of decay for pin-jointed frameworks consisting of a series of identical repeated cells, and re-considered examples originally treated by Hoff [7]. Nodal displacements and forces on either side of the generic single cell are considered as state variables and are

† If a matrix has repeated eigenvalues, it is not diagonalizable unless it has a full set of independent eigenvectors. If the eigenvectors are not independent then it can only be reduced to a block form and the original matrix is said to be *defective*. It is *derogatory* if the same eigenvalue appears in more than one block.

related by a transfer matrix which may be readily determined from a knowledge of the cell stiffness matrix (which in turn may be found by a variety of means). Assuming consecutive state vectors to be related by a constant multiple λ (which is the decay factor) leads directly to an eigenvalue problem. For decaying modes, associated with self-equilibrated loads, the eigenvalues occurs as reciprocal pairs (that is, if λ_n is an eigenvalue then so is $1/\lambda_n$) according to whether decay is from left-to-right or *vice-versa*. Rigid body displacements have $\lambda = 1$, as do the transmitting eigenmodes pertaining to nodal load distributions which do constitute a force or moment resultant. However since the transfer matrix is both *defective* and *derogatory*†, it is necessary to use the rigid body eigenvectors to generate the principal vectors for the transmitting modes. The matrix of eigen- and principal vectors then forms a similarity matrix which transforms the original transfer matrix into Jordan canonical form. Bi-orthogonality properties of the eigenvectors then allow modal

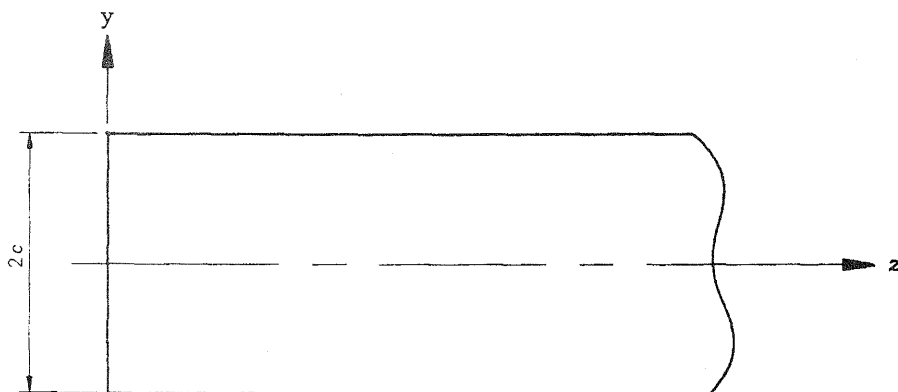


Fig. 2. Semi-infinite plane strain strip.

Table 1. Decay rates, k_c , for the plane strain strip: (s) and (a) denote symmetric and asymmetric loadings, respectively

| Model 1 | Model 2 | Model 3 | Model 4 | Model 5 | Exact |
|------------------------|------------------------|------------------------|------------------------|-------------------------|----------------------------|
| 2.1095062 ± 1.1760995i | 2.1073316 ± 1.1379524i | 2.1063227 ± 1.1282564i | 2.1063339 ± 1.1254489i | 2.1062059 ± 1.1253805i | 2.1061961 ± 1.1253643i(s) |
| 3.8553844 ± 1.6104521i | 3.7772316 ± 1.4371533i | 3.7564987 ± 1.3976780i | 3.7500251 ± 1.3841426i | 3.7489152 ± 1.3843019i | 3.7488381 ± 1.3843391i(a) |
| 5.7825589 ± 2.1551664i | 5.4637258 ± 1.6785047i | 5.3822262 ± 1.5828351i | 5.3587542 ± 1.5485655i | 5.3568295 ± 1.5573551i | 5.3562687 ± 1.5515744i(s) |
| | 7.2180233 ± 1.9184778i | 7.0182967 ± 1.7365523i | 6.9378010 ± 1.6658117i | 6.9487169 ± 1.6756548i | 6.9499798 ± 1.6761049i(a) |
| | 9.0824633 ± 2.1821724i | 8.7806005 ± 1.9699534i | 8.4068293 ± 1.7727961i | 8.5370320 ± 1.7737923i | 8.5366824 ± 1.7755437i(s) |
| | | | | 10.1494624 ± 1.8497912i | 10.1192588 ± 1.8583838i(a) |
| | | | | 11.6823196 ± 1.9578636i | 11.6991776 ± 1.9294045i(s) |
| | | | | | 13.2772736 ± 1.9915708i(a) |

decomposition of an arbitrary end load. As a by-product of the work in Ref. [6] it was also possible to determine exactly the "continuum" beam properties of the framework, such as equivalent cross-sectional area, Poisson's ratio, second moment of area and shear coefficient, which can be very useful in preliminary design work.

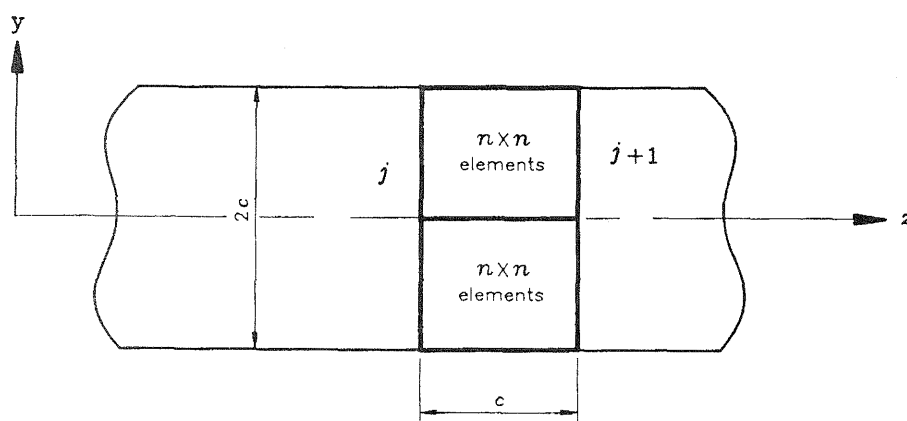
In the present paper this procedure for the pin-jointed framework is developed for a continuum prismatic beam or rod of arbitrary cross-section. The beam is considered to consist of a series of identical sections of appropriate length (related to a characteristic cross-sectional dimension), and the stiffness matrix is formulated within ANSYS finite element code. Since nodal displacements and forces within the beam section are not required for the eventual transfer matrix, these nodes are treated as *slave* nodes, whilst the nodes at the two section ends are treated as *master* nodes; this is readily accomplished within ANSYS using the *super element*†. Once the *super element* stiffness matrix has been formulated, it is imported into a MATLAB environment wherein the manipulations to form the transfer matrix, and determination of the eigenvalues using a reliable QR algorithm, is easily accomplished.

Accuracy of the method is assessed by treating the plane strain strip (see Ref. [8], article 26), the plane strain sandwich strip [9], and the beam of circular cross-section [10], which are representative of the few exact (within the spirit of the linear mathematical theory of elasticity) analytical solutions available for the so-called *end* problem.

THEORY

We consider a prismatic elastic cylinder of arbitrary cross-section and semi-infinite length subjected to a self-equilibrated loading on the end $z = 0$, Fig. 1, and suppose that it may be divided into a series of consecutive identical sections of finite length l_c , which is taken to be a characteristic dimension of the cross-section, for example the radius b in the case of a cylinder of circular cross-section. The cross-sections to the left and right of the j th such section are denoted as the j th and $(j + 1)$ th, respectively, and the typical nodal force and displacement directions on the j th section are shown. Some, but not necessarily all, of these cross-sectional nodes may be *master* nodes, which connect to the adjoining $(j - 1)$ th and $(j + 1)$ th sectional lengths; such nodes bear the subscript m . Nodes within the j th sectional length, and any nodes on the section ends which are not *master* nodes, are termed *slave* nodes and bear the subscript s . For the complete sectional length l_c the nodal

† The condensation of a group of finite elements into just one *super element*, represented as a matrix known as a sub-structure, is normally employed to reduce computer time and also to allow solution of large problems with limited computer memory resources.





| | Division of c | Element type | $c = 1$ |
|---------|-----------------|--------------|---|
| MODEL 1 | $n=5$ | 4 node |  $E = 2 \times 10^5 \text{ N/mm}^2$ $\nu = 0.25$ |
| MODEL 2 | $n=10$ | 4 node | |
| MODEL 3 | $n=20$ | 4 node | |
| MODEL 4 | $n=5$ | 8 node |  |
| MODEL 5 | $n=10$ | 8 node | |

Fig. 3. Sectional length models for plane strain strip.

(master and slave) forces and displacements are related by means of the stiffness matrix $[K]$ as

$$[K]\{u\} = \{F\}. \quad (1)$$

This equation may be suitably partitioned as

$$\begin{bmatrix} [K_{m,m}] & [K_{m,s}] \\ [K_{s,m}] & [K_{s,s}] \end{bmatrix} \begin{Bmatrix} \{u_m\} \\ \{u_s\} \end{Bmatrix} = \begin{Bmatrix} \{F_m\} \\ \{F_s\} \end{Bmatrix} \quad (2)$$

Expanding and re-arranging, eqn (2) may be expressed as

$$[\hat{K}]\{\hat{u}\} = \{\hat{F}\}, \quad (3)$$

where

$$[\hat{K}] = [K_{m,m}] - [K_{m,s}][K_{s,s}]^{-1}[K_{s,m}]$$

$$\{\hat{F}\} = \{F_m\} - [K_{m,s}][K_{s,s}]^{-1}\{F_s\}$$

$$\{\hat{u}\} = \{u_m\}.$$

Here $[\hat{K}]$ is the stiffness matrix of the sectional length treated as a *super element*, $\{\hat{u}\}$ is the column vector of displacements of the *master* nodes, and $\{\hat{F}\}$ is the column vector of forces applied to the *master* nodes on the end cross-sections. Such a *super element* stiffness matrix can be readily formulated within ANSYS.

The matrix eqn (3), together with the force and displacement vectors pertaining to the *super element* can now be partitioned according to whether the forces and displacements components are left hand j th or right hand $(j+1)$ th sides, as

$$\begin{Bmatrix} \hat{F}_j \\ \hat{F}_{j+1} \end{Bmatrix} = \begin{bmatrix} \hat{K}_{j,j} & \hat{K}_{j,j+1} \\ \hat{K}_{j+1,j} & \hat{K}_{j+1,j+1} \end{bmatrix} \begin{Bmatrix} \hat{u}_j \\ \hat{u}_{j+1} \end{Bmatrix}. \quad (4)$$

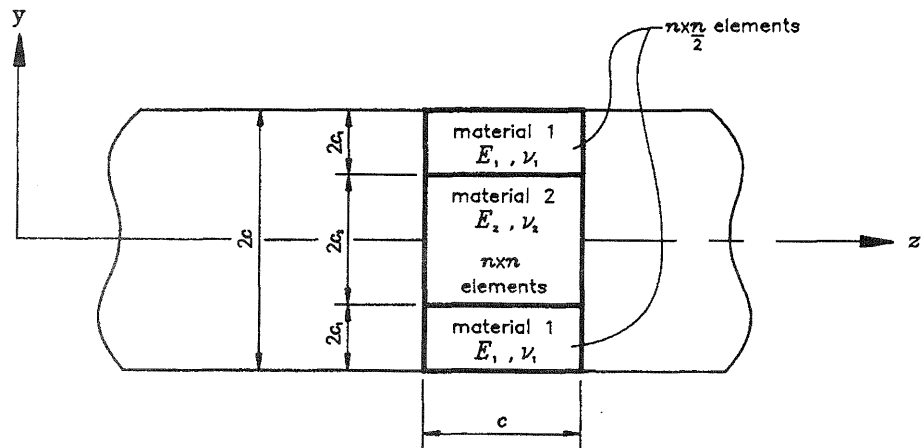
Lastly we write $\hat{F}_j = -p_j$, $\hat{F}_{j+1} = p_{j+1}$, $\hat{u}_j = d_j$, $\hat{u}_{j+1} = d_{j+1}$, where a minus sign has been introduced to conform with the force conventions of the transfer matrix method† (rather than the finite element method), and again expand and re-arrange to give

$$\begin{Bmatrix} d_{j+1} \\ p_{j+1} \end{Bmatrix} = \begin{bmatrix} -\hat{K}_{j,j+1}^{-1} \hat{K}_{j,j} & -\hat{K}_{j,j+1}^{-1} \\ \hat{K}_{j+1,j} - \hat{K}_{j+1,j+1} \hat{K}_{j,j+1}^{-1} \hat{K}_{j,j} & -\hat{K}_{j+1,j+1} \hat{K}_{j,j+1}^{-1} \end{bmatrix} \begin{Bmatrix} d_j \\ p_j \end{Bmatrix} \quad (5)$$

or

† Positive forces are defined according to the conventions of the theory of elasticity.

$$s_{j+1} = Gs_j, \quad (6)$$




| | Division of c | Element type | $c=1$ |
|---------|-----------------|--------------|--|
| MODEL 1 | $n=6$ | 8 node |  $E_1 = E_2 = 2 \text{ E } 05 \text{ N/mm}^2$ |
| MODEL 2 | $n=10$ | 8 node | |

Fig. 4. Sectional length models for plane strain sandwich strip.

where $s_j = \{d_j, p_j\}^T$ and $s_{j+1} = \{d_{j+1}, p_{j+1}\}^T$, T denotes the transpose, and G is the transfer matrix.

Now the piecewise equivalent of exponential decay is that nodal forces should be reduced by a constant factor λ as one moves from cell to cell; similarly consideration of the Hooke's laws would suggest that the nodal displacements associated with the self-equilibrated load should also decay from cell to cell in a similar manner. We therefore set

$$s_{j+1} = \lambda s_j. \quad (7)$$

Substituting the above into eqn (6) gives

$$\lambda s_j = G s_j, \text{ or } [G - \lambda I] s_j = 0. \quad (8)$$

Thus the decay factors λ are the eigenvalues of the transfer matrix G ; the associated eigenvectors give

the j th section nodal displacements and loads for the particular decay mode.

Since the ratio of *master* nodal forces p on the $(j+1)$ th and j th sections is λ , an equivalent exponential decay rate may be determined as

$$\lambda = \frac{p_{j+1}}{p_j} = \frac{p_0 e^{k(j+1)}}{p_0 e^{kj}} = e^k, \text{ or } k = \ln(\lambda). \quad (9)$$

EXAMPLES

Plane strain strip

The exact solution for the plane strain strip, due to Papkovitch and Fadle (see Ref. [8], article 26), has stress decaying from the loaded edge as $\exp(-kz)$

Table 2. Decay rates, $k(2c_1 + c_2)$, for the sandwich strip

| Present method | | Choi and Horgan (exact) | |
|---------------------------------|---------------------------------|----------------------------|----------------------------|
| $\nu_1 = 0.2, \nu_2 = 0.4$ | $\nu_1 = 0.4, \nu_2 = 0.2$ | $\nu_1 = 0.2, \nu_2 = 0.4$ | $\nu_1 = 0.4, \nu_2 = 0.2$ |
| (I) $2.0572647 \pm 1.2846068i$ | (I) $2.1565728 \pm 0.9562300i$ | $2.057207 \pm 1.284533i$ | $2.156514 \pm 0.956221i$ |
| (II) $2.0572187 \pm 1.2845427i$ | (II) $2.1565401 \pm 0.9562355i$ | | |

(I) denotes Model 1, (II) denotes Model 2.

Table 3. Data for circular section rod models in Fig. 6

| Model | Division of b | Division of l_c | Element type | No. of elements | No. of nodes | Transfer matrix |
|-------|-----------------|-------------------|---------------|-----------------|--------------|--------------------|
| 1 | 2 | 2 | 8 node brick | 24 | 51 | (102×102) |
| 2 | 4 | 4 | 8 node brick | 192 | 285 | (342×342) |
| 3 | 2 | 4 | 20 node brick | 48 | 225 | (270×270) |
| 4 | 3 | 4 | 20 node brick | 80 | 345 | (414×414) |

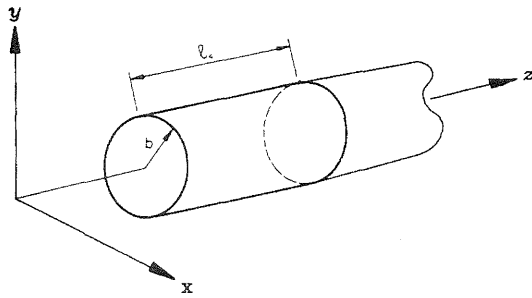


Fig. 5. Semi-infinite rod of solid circular cross-section.

where, for the strip of depth $2c$, Fig. 2, the eigenequation governing decay rate k is

$$\sin 2kc \pm 2kc = 0; \quad (10)$$

the positive and negative signs correspond to loads symmetric and asymmetric, respectively, about the z -axis. The first eight roots are shown in Table 1.

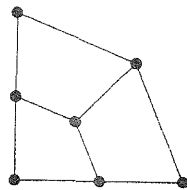
For the numerical analysis, five models of length unity and depth two were constructed on ANSYS as shown in Fig. 3, employing four-node or eight-node plane isoparametric elements, and the results are shown in Table 1. Firstly we note that a blank entry in the table does not indicate that an eigenvalue was not found but rather that it was too inaccurate to be obviously identified as close to an exact eigenvalue, in which case consideration of the associated

eigenvector, which would facilitate identification, was not thought worthwhile.

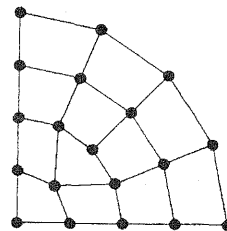
The simplest Model 1 provides an excellent approximation to the slowest decay rate (first symmetric) in which the real part, which governs the rate of decay, is just 0.16% too large, while the second decay rate (first asymmetric) is 2.84% too large. At the other extreme the most complicated Model 5 is able to predict the first seven decay rates (real part) to within an accuracy of better than 0.3%; the smallest eigenvalue, which provides the validation of S.V.P. is almost exact. Comparing the predictions of Model 3 and Model 5, which both lead to a stiffness matrix of equal magnitude, it is clear that the eight-node element is superior. The same conclusion is reached when comparing Models 2 and 4.

Plane strain sandwich strip

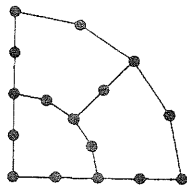
The extension of the Papkovitch-Fadle strain solution to the case of a symmetric sandwich consisting of two isotropic materials was considered in Ref. [9] wherein the authors warned against the routine invocation of S.V.P. in the case of sandwich, composite and highly anisotropic materials. The solution was constructed using an *Airy* stress function and the eigenequation governing decay rates arose from the boundary requirements that the face and core be perfectly bonded at the interface, and that the upper and lower surfaces be free of traction, Fig. 4.



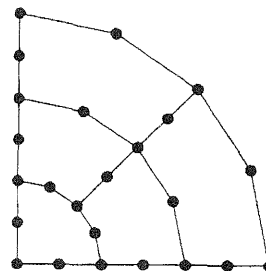
MODEL 1



MODEL 2



MODEL 3



MODEL 4

Fig. 6. Sectional length models for solid circular cross-section rod: division of cross-section. Only one quarter of cross-section is shown.

Table 4. Decay rates, kb , for the solid circular section rod; m is the circumferential harmonic index [see eqn (11)]

| Model 1 | Model 2 | Model 3 | Model 4 | Exact |
|------------------------|------------------------|------------------------|------------------------|------------------------------------|
| 2.2053805 ± 1.3123340i | 2.1427899 ± 1.0418212i | 2.1048326 ± 0.9642468i | 2.1048037 ± 0.9621763i | 2.1043544 ± 0.9592205i ($m = 2$) |
| 2.5765032 ± 2.1647539i | 2.7134593 ± 1.5759504i | 2.7133699 ± 1.3715151i | 2.7039049 ± 1.3681677i | 2.6976518 ± 1.3673570i ($m = 0$) |
| 2.7460418 | 2.9973139 | 2.8063505 | 2.8026211 | 2.7931415 ($m = 1$) |
| 3.3239616 ± 1.6595336i | 3.4353848 ± 1.4036251i | 3.2750160 ± 1.1971660i | 3.2832025 ± 1.1927975i | 3.2858613 ± 1.1576914i ($m = 3$) |
| | | 4.2233419 | 4.1974044 | 4.0882060 ($m = 2$) |
| | | 4.1504193 ± 1.4484321i | 4.1896002 ± 1.5293183i | 4.2852175 ± 1.4981961i ($m = 1$) |
| | | 4.3788850 ± 1.5384929i | 4.3190350 ± 1.5017550i | 4.4047845 ± 1.3040193i ($m = 4$) |
| | | 5.271012 | 5.1552161 | 5.1356223 ($m = 0$) |
| | | | 5.2957151 ($m = 3$) | 5.2957151 ($m = 3$) |
| | | | 5.7952914 ± 1.6698540i | 5.6799579 ± 1.6129679i ($m = 2$) |
| | | | | 6.0512222 ± 1.6381471i ($m = 0$) |
| | | | | 6.4629421 ($m = 4$) |

The relative thickness of the face material compared with the core was characterized by the non-dimensional parameter (volume fraction)

$$f = \frac{4c_1}{4c_1 + 2c_2}.$$

For the present comparison we choose a sandwich strip for which $f = 1/2$, and the two materials have identical Young's modulus E but differing Poisson's ratio ν . The results are shown in Table 3 for two different models both employing eight node plane elements, and again the agreement is seen to be very good.

Cylinder of circular cross-section

The most complete analysis of the solid circular section has been provided by Klemm and Little [10]. This was extended by Stephen and Wang [11] for the hollow circular cross-section, who considered the self-equilibrated end load problem, assuming displacements to decay exponentially with axial coordinate z and to be periodic in angular coordinate θ , that is

$$(u_r, u_\theta, u_z) = (U(r), iV(r), W(r)) \exp(im\theta - kz). \quad (11)$$

The solution was constructed using the formal Papkovitch-Neuber solution to the (Navier) displacement equations of equilibrium; the requirement of zero stresses on the surface generators leads to an eigen-determinant of sixth order, whose elements involve either Bessel or Neumann functions. The decay rate is thus expressed as a multiple of the external radius b . The sixth order determinant reduces to the same eigenequation as derived by Klemm and Little for the solid section when the Neumann functions and associated constants are excluded.

For the numerical analysis, four models were constructed on ANSYS as shown in Fig. 6, employing eight-node or 20-node brick elements; data for these models are shown in Table 3. The radius and section length are both taken as unity. The results are shown in Table 4† together with the first 12 exact decay rates. Again blank entries indicate eigenvalues which are too inaccurate to warrant study of the associated eigenvectors.

Comparing the predictions of Models 2 and 3 it is immediately obvious that the eight-node brick element of Model 2, which leads to a larger transfer matrix, is inferior to the 20-node element of Model 3. Model 4 predicts the real part of the slowest decay rate to an accuracy of 0.02% error, and the first four decay rates to an accuracy of better than 0.5% error.

† Where, by virtue of the symmetry of the cross-section, two near identical eigenvalues are obtained, the average value is shown.

CONCLUSIONS

A numerical procedure previously developed to determine the "exact" decay rates for the idealized pin-jointed framework consisting of repeated identical cells is here further developed to allow application to the prismatic continuum rod or beam of general cross-section. Comparison with available exact elasticity solutions shows that the method is capable of providing decay rate predictions to a very high accuracy, for both a single isotropic material and for a sandwich construction of two different isotropic materials.

Acknowledgement—The authors give special thanks to M. Street of the Central Design Service of Southampton University for preparation of the drawings.

REFERENCES

1. I. S. Sokolnikoff, *Mathematical Theory of Elasticity*, 2nd Edn. McGraw-Hill, New York (1956).
2. R. A. Toupin, Saint-Venant's principle. *Arch. Rat. Mech. Anal.* **18**, 83–96 (1965).
3. V. V. Vlasov, *Thin Walled Elastic Beams*, 2nd Edn. The Israel Program For Scientific Translation (1961).
4. C. O. Horgan and J. K. Knowles, Recent developments concerning Saint-Venant's principle. In: *Advances in Applied Mechanics* (Edited by J. W. Hutchinson), Vol. 23, pp. 179–269. Academic Press, London (1983).
5. C. O. Horgan, Recent developments concerning Saint-Venant's principle: an update. *ASME appl. Mech. Rev.* **42**, 295–303 (1989).
6. N. G. Stephen and P. J. Wang, On Saint-Venant's principle for the pin-jointed framework. *Int. J. Solids Struct.* (in press).
7. N. J. Hoff, The applicability of Saint-Venant's principle to airplane structures. *J. Aeronaut. Sci.* **12**, 455–460 (1945).
8. S. P. Timoshenko and J. N. Goodier, *Theory of Elasticity*, 3rd Edn. Article 26. McGraw-Hill, New York (1970).
9. I. Choi and C. O. Horgan, Saint-Venant end effects for plane deformation of sandwich strips. *Int. J. Solids Struct.* **14**, 187–195 (1978).
10. J. L. Klemm and R. W. Little, The semi-infinite elastic cylinder under self equilibrated end loading. *SIAM J. appl. Math.* **19**, 712–729 (1970).
11. N. G. Stephen and M. Z. Wang, Decay rates for the hollow circular cylinder. *ASME J. appl. Mech.* **59**, 747–753 (1992).